

Vegetation clustering and self-organization in inhomogeneous environments

D. Pinto-Ramos^{1,2}, M. G. Clerc², A. Makhoute³, and M. Tlidi⁴

¹*Center for Advanced Systems Understanding (CASUS); Helmholtz-Zentrum Dresden-Rossendorf (HZDR), D-02826 Görlitz, Germany*

²*Departamento de Física and Millennium Institute for Research in Optics, Facultad de Ciencias Físicas y Matemáticas, Universidad de Chile, Casilla 487-3, Santiago, Chile*

³*Faculté des Sciences, Université Moulay Ismail, Dynamique des Systèmes Complexes, B.P. 11201, Zitoune, Meknès, Morocco*

⁴*Faculté des Sciences, Université Libre de Bruxelles (U.L.B), CP. 231, Campus Plaine, B-1050 Bruxelles, Belgium*

Abstract

Due to climatic changes, excessive grazing, and deforestation, semi-arid and arid ecosystems are vulnerable to desertification and land degradation. Adversely affected biological productivity has a negative impact on social, economic, and environmental factors. The term "arid ecosystems" refers not only to water-scarce landscapes but also to nutrient-poor environments. Specifically, the vegetation cover loses spatial homogeneity as aridity increases, and the self-organized heterogeneous vegetation patterns developed could eventually collapse into a bare state. It is still unclear whether this transition would be gradual or abrupt, leading to the often-called catastrophic shift of ecosystems. Several studies suggest that environmental inhomogeneities in time or space can promote a gradual transition to bare soil, thus avoiding catastrophic shifts. Environmental inhomogeneities include non-uniformities in the spatial distribution of precipitation, spatial irregularities in topography and other external factors. Employing a generic mathematical model including environmental inhomogeneities in space, we show how two branches of vegetation patterns create a hysteresis loop when the effective mortality level changes. These two branches correspond to qualitatively distinct vegetation self-organized responses. In an increasing mortality scenario, one observes an equilibrium branch of high vegetation biomass forming self-organized patterns with a well-defined wavelength. However, reversing the mortality trend, one observes a low biomass branch lacking a wavelength. We call this phenomenon the clustering of vegetation patches. This behavior can be connected to historically significant trends of climate change in arid ecosystems.

Introduction

Semi-arid and arid landscapes are particularly vulnerable to climate change and desertification. Considering they cover up to 45 percent of the Earth's terrestrial surface, several studies have investigated how environmental changes cause uniform vegetation cover to shift into a patchy landscape [1, 2, 3, 4, 5]. It is widely

accepted that symmetry-breaking instability mediated by two opposite feedbacks (facilitation and competition) acting on different spatial scales, causes this transition even in homogeneous environments [1]. The resulting self-organized structures, are commonly called vegetation patterns, and correspond to a heterogeneous distribution of the biomass across space. These coherent structures are modified by precipitation gradients, suggesting that

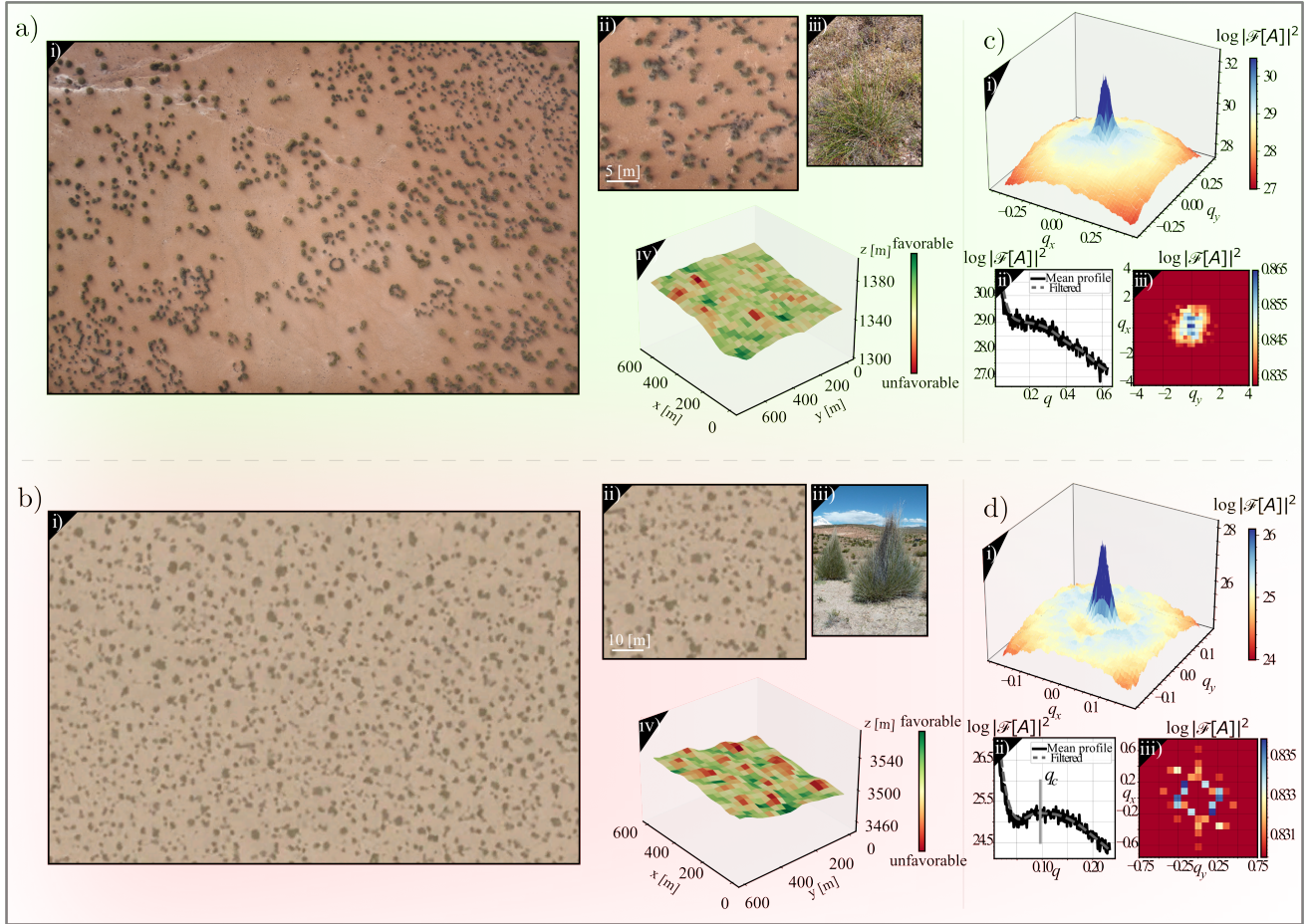


Figure 1: Clustered and self-organized vegetation patches. a) Morocco, Enjil region (Boulmane Province) $18^{\circ} 49.3'S$, $35^{\circ} 37.4'E$., patches formed by alpha or *Stipa tenacissima L.* plants in i), ii), and iii). b) Argentina (Catamarca, northwestern Argentina plateau) $23^{\circ} 25.8'S$, $66^{\circ} 4.4'W$. Patches formed by paja brava or *Fetusca orthophylla* plants in i), ii), and iii). Panels iv) indicate the topographic profile, with colors highlighting the local minima (green) and maxima (red) of the respective landscape. Panels c-i) and d-i) illustrate the 2D Fourier spectrum of the vegetation cover field, and panels ii) and iii) depict the mean profile of the 2D Fourier spectrum in the radial direction and the windowed Fourier spectrum of each ecosystem, respectively.

ecosystems can undergo structural changes as the factors regulating these structures vary [2, 6].

Arid ecosystems are characterized by having potential evapotranspiration (PET_0) exceeding the water supply provided by rainfall (P) annually. More precisely, the aridity is defined as $Ar = 1 - P/PET_0$, not to be confused with the typical aridity index $AI = P/PET_0$. Reduced precipitation and increased evapotranspiration rates or,

equivalently, increased aridity directly impact vegetation function [7, 8]. As environmental adversity increases, a homogeneous cover becomes degraded and gives rise to gaped, then stripes (or labyrinths) and patches before collapsing onto the bare ground [9, 10]. This generic sequence has been found in other modeling approaches incorporating water transport [4, 11, 12]. In addition to periodic biomass distributions, localized patches of

vegetation were observed [13, 14] or localized labyrinths [15], as well as arcs, spirals [16], pulses [17], and multistable domains of oblique stripes [18]. In addition, another mechanism associated with the phenomenon of non-equilibrium phase separation can generate vegetation patterns in the form of non-random biphasic structures [19, 20, 21, 22]. Modeling vegetation patterns in strictly homogeneous environments has attracted a lot of interest, but patterns that settle in spatially inhomogeneous environments are increasingly being studied due to the relevance of inhomogeneities in the vegetation biomass output and resilience to increased environmental stress [23, 24, 25, 26, 27].

In natural ecosystems, spatial inhomogeneities in environmental conditions are the rule rather than the exception. Spatial inhomogeneities encompass non-uniformities in the spatial distribution of precipitation, soil properties such as spatial irregularities in topography [28, 29], soil depth [30] or moisture islands [31], atmospheric factors such as wind and light, or even grazing and fire episodes [32, 33, 30, 31, 34], and human activities [35]. Studies that take into account spatiotemporal [36] and temporal [37] fluctuations in vegetation models produce time-varying biomass distributions that can elude the turning points existing in the homogeneous theory. Similarly, spatial inhomogeneities induce equilibrium distributions that can also elude tipping points [24]. These investigations support the prediction of irregular vegetation distributions.

Here, we use field measurements, remote sensing image analysis, and a well-known model to study the formation of vegetation patches on bare ground with topographic irregularities. We unveil how the static spatial environmental inhomogeneities, such as the variations in the topography, affect the biomass density distribution. We show evidence of two types of vegetation patterns that form a hysteresis loop as a function of the aridity level. These two branches of equilibria generated by inhomogeneities represent qualitatively distinct vegetation patterns. They can be distinguished not only through their average biomass [24], but also by using the spatial Fourier spectrum and the pair correlation function. As the aridity level increases, the ecosystem develops self-organized patterns with a well-defined wavelength. However, when the aridity level is reversed, the vegetation pattern undergoes a clustering phenomenon without a wavelength. By combining remote sensing im-

age analysis and the rate of change of aridity worldwide, we link our prediction to significant historical trends of climate change in arid ecosystems. In addition, we recover the observation that the transition from a patchy ecosystem to bare soil is quite smooth and gradual in the presence of spatial inhomogeneities, thus avoiding catastrophic shifts [37, 38, 39, 40, 41, 42]. Understanding the formation of vegetation patterns under inhomogeneous environmental conditions increases the possibility of successfully conserving and maintaining vegetation in arid ecosystems. Remarkably, inhomogeneous environmental conditions allow for vegetation patches with an aperiodic distribution in space as a stable equilibrium, namely, the clustering of patches branch of solutions. This is different than homogeneous systems, where an aperiodic patch distribution is only transient due to the repulsive interaction of the localized structures [43], leading to periodic structures as equilibria.

Field observations and remote sensing image analysis

Self-organization versus clustering

We consider vegetation patches distributed within a bare soil matrix. Two examples of patchy landscapes taken from Morocco and Argentina are shown in Figs. 1a) and 1b), respectively. The two ecosystems are located in a high-altitude arid zone with complex topographical variations around a gentle, mean slope, as shown in Figs. 1a)iv) and 1b)iv) [44]; the color accounts for variations due to topography indicated by the local maxima (red) and minima (green), namely, it describes the spatial variation of the slope [29]. These plant populations develop on soil with spatial irregularities. The vegetation shown in Morocco corresponds to *Stipa tenacissima* L., often called alfa, originally from northwestern Africa and the southern part of the Iberian Peninsula. This plant belongs to a species of monocotyledonous plants in the Poaceae family [16, 45]. To this family belongs *Festuca orthophylla* shown in the northwestern Argentina plateau [cf. Fig. 1b)]. Both clonal vegetation patches grow on dry, rocky, base-rich soils, forming a steppe-like grassland. In these harsh environments, vegetation patches in high mountain ecosystems have to face a high degree of aridity as well as low minimum temperatures that limit their development, and they often experience graz-

ing pressure from ruminants. Contrary to most alpine environments, these landscapes may become drier due to the lack of persistent snow cover [46, 47].

It is now generally accepted that plant facilitative and competitive interactions can lead to self-organized vegetation patterns [1, 48]. Two feedback operating at different spatial scales are required for this process to take place. The positive feedback associated with the facilitative interaction, which operates at the level of the plant size L_f , tends to increase the total biomass (activator) of surrounding plants. On the other hand, negative feedback linked to the competitive interaction (inhibitor) between plants is also included. This interaction operates at the plant roots size L_c level and tends to inhibit the biomass growth of surrounding plants up to a distance L_c . Field observations for two different plants have validated this modeling approach: *Combre-tum micranthum* [49, 50, 51] and *Festuca orthophylla* [52]. *Festuca orthophylla* plant shares many characteristics with the alfa plant. Field measurements indicate that the density of the alfa plant is 0.44 tufts per m^2 and that the total above-ground dry biomass reached 873 grams per tuft [16, 45]. The alfa or *Stipa tenacissima* *L.* patches reach a mean radius of $L_f \approx 57$ cm, with roots extending in a mean radius of $L_c \approx 180$ cm. Similarly, vegetation observed in the northwestern Argentina plateau, *Festuca orthophylla*, is characterized by forming patches-like structures of several individuals, having a mean structure radius of $L_f \approx 50$ cm and mean root extension of $L_c \approx 140$ cm [52]. Both plants survive in low rainfall environments, reaching mean aridity levels of 0.65 and 0.70 [53], respectively.

Models based on facilitation on competition relate the existence of a periodic pattern with the ratio of facilitation to competition length L_f/L_c [50, 54]. Interestingly, plants *Stipa tenacissima* *L.* and *Festuca orthophylla* share similar structural properties and aridity levels, both having a facilitation to competition length $\sim 1/3$, then, it is expected to observe the same type of self-organization due to the environmental stress. To analyze the patches' spatial distribution, we use the spatial Fourier transform together with the pair correlation function of the patches' positions. These tools help to clarify and categorize the different spatial self-organizations of vegetation patches. We compute the spatial Fourier transform for *Stipa tenacissima* *L.* and *Festuca orthophylla* remote sensing images, which are binarized to

highlight vegetation from soil (see supplementary materials), and corresponding to areas of $0.14km^2$ and $0.84km^2$, respectively. The results are shown in Figs. 1c) and 1d). The amplitude of the spatial Fourier transform reveals a significant difference in the spatial organization of these vegetation patches. *Stipa tenacissima* *L.* patches have the $q = 0$ mode as dominant [see Fig. 1c) (i)]. Differently, the *Festuca orthophylla* patches exhibit a ringed region of local maxima at $q \neq 0$ [see Fig. 1c) (ii)] corresponding to the pattern wavelength [55]. This difference can be highlighted by computing the radial profile of these spatial Fourier transform amplitudes as $\mathcal{F}[A](x, y) = \mathcal{F}[A](q, \theta) \approx \langle \mathcal{F}[A](q) \rangle_\theta$, where $\langle \cdot \rangle_\theta$ is the average over θ (see supplementary materials for details). A is the binarized reflected light intensity field of the images. This method enables one to distinguish whether a local maximum exists at $q \neq 0$ or not, as shown in Figs. 1c)ii) and 1d)ii). The lack of a pattern structure for *Stipa tenacissima* *L.* patches distribution is seen in the local Fourier transform [56] amplitude Fig. 1c)iii). *Festuca orthophylla*, on the other hand, has a locally distinctive hexagonal pattern shown in Fig. 1d)iii).

The presence or absence of the wavelength is not specific to clonal vegetation patches observed in high mountain ecosystems. It can be found in many other patchy ecosystems with different types of plants and soils. Eight ecosystems worldwide are depicted in Figure2a), where vegetation patches' spatial distribution can be categorized as either having a characteristic wavelength or not. The images were obtained using the Google Earth Pro program from locations in the United States, Argentina, Zambia, Mozambique, India, and Australia. To capture photographs of patterns in Morocco, smart drone photography was employed since the resolution of satellite images was inadequate. The radial profile of the Fourier transform of the patchy landscapes is shown in Fig. 2b). The vegetation of the USA, Argentina, India, and southeast Australia shows self-organization with a well-defined characteristic wavelength in addition to the zero wavenumber [see the red curves of Fig.2b)]. The green curves in this figure indicate that the vegetation patterns observed in Morocco, Zambia, Mozambique, and northwest Australia do not have a characteristic wavelength, and only the zero wavenumber dominates the spatial distribution of patches. The pair correlation function of the patch centers is computed, as shown in Fig. 2c). The green curves show that the patterns with-

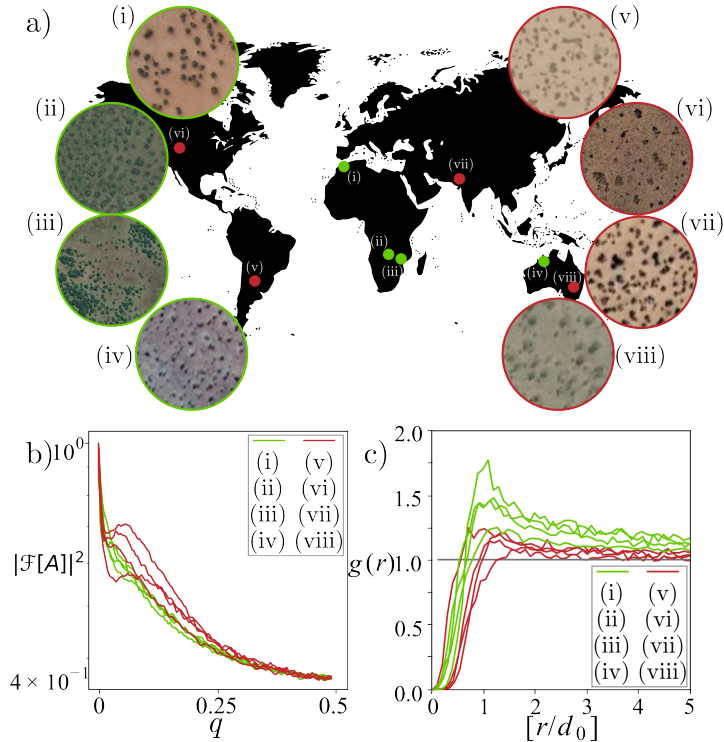


Figure 2: Vegetation patchy landscape classification in different locations of the world employing remote sensing analysis. a) Clustered and self-organized vegetation patches across the planet. Red and green frames [(i)-(viii)] account for self-organized and clustered patches, respectively. The red and green dots [(i)-(viii)] in the map stand for the respective location under study. b) The mean profile of the 2D Fourier spectrum of each vegetation pattern depicted in the a) panel; the red and green curves indicate the presence or absence of a characteristic wavelength. c) Corresponding pair correlation function of each patchy landscape.

out a distinctive wavelength have higher correlations in their relative separations from patches at closer distances compared to the red curves.

The global trend map as an indicator of ecosystem self-organization and clustering

The observation of two different types of self-organized spots opens the question of their origin. An aperiodic distribution of spots to be observed in a homogeneous system would require fine-tuning and the observation of transient states [57]. However, under inhomogeneous environmental conditions, aperiodic distributions of spots can appear naturally just by changing environmental conditions over time. Thus, the observation of either pe-

riodic or aperiodic vegetation patches could be related to the history of environmental conditions. Fourier transforms of the vegetation patterns and the pair correlation function of patch positions let us classify whether an ecosystem operates in the self-organized or clustering behavior. Further, using a database of bio-climatic indicators [53], we collect two meteorological variables that are crucial for patch formation and assessments of aridity: the mean annual precipitation (P) and the reference potential evapotranspiration (PET_0). These quantities are available in this database with global coverage and a resolution of 0.5° in the polar and azimuthal axes of the planet. Let us assume that the mortality is a growing function of the aridity $Ar = 1 - P/PET_0$. Then, we compute a global trend map of the vegetation envi-

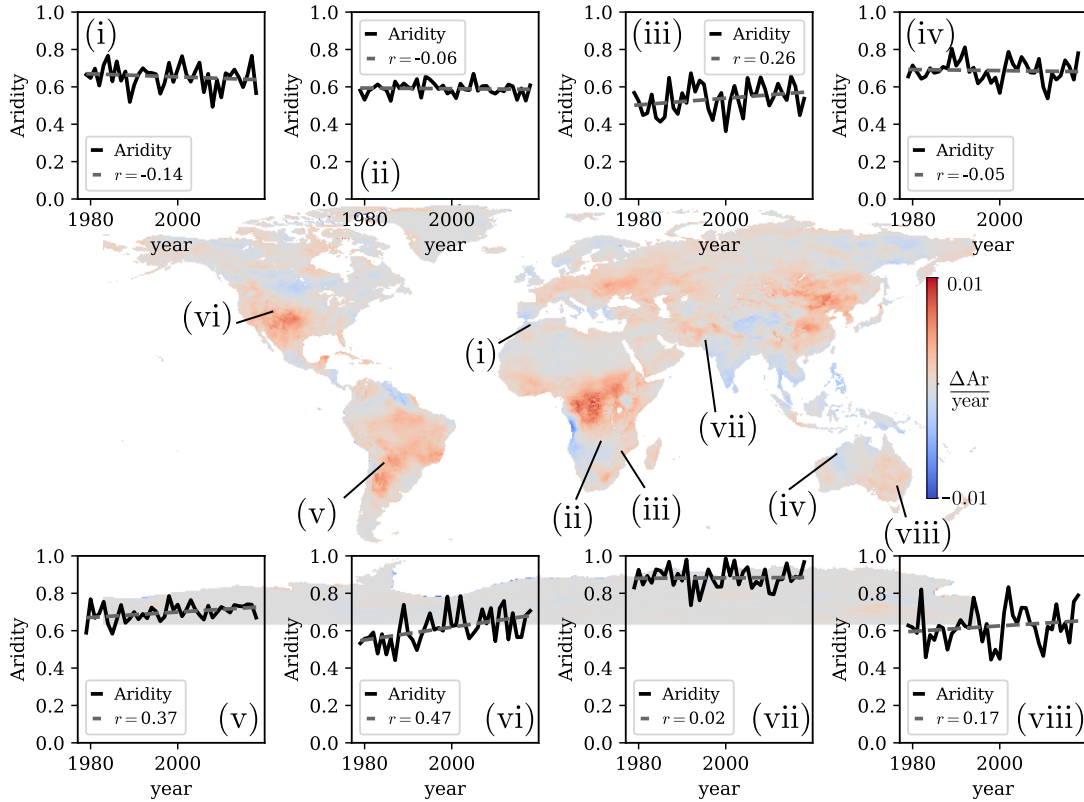


Figure 3: Change rate in the aridity worldwide extracted from linear regression. Blue (red) regions show the landscapes in which the aridity has decreased (increased) from 1979 to 2018. In the map, the landscapes analyzed are signaled by arrows. Insets show the aridity trend over the years and the Pearson correlation coefficient. Mosaics of vegetation from Morocco, USA, Argentina, Zambia, and Australia agree with the theory developed; The mosaics of Mozambique show the opposite tendency described by the theory.

ronmental conditions temporal gradient. The results are shown in Fig. 3. The areas shown in red indicate an average increase in aridity over the years. The ecosystems of Argentina, USA, India, and South of Australia are characterized by increasing aridity, as shown in Figs. 3(V, VI, VII, VIII), respectively. These ecosystems exhibit a self-organized spatial distribution of biomass with a well-defined wavelength. The blue zones indicate areas where aridity has decreased on average over the years. Ecosystems from Morocco, Zambia, and North Australia have been subjected to a decrease in the aridity, as shown in Figs 3(I, II, V), respectively. These ecosystems exhibit a clustering phenomenon, a vegetation cover without wavelength.

It is reasonable to think that the vegetation pattern could have experienced changes thanks to the variation of aridity over time, affecting plant growth. A signature of this change could be the spatial distribution of the vegetation cover, it being either self-organized (with a dominant wavelength), or clustered (without wavelength). However, according to data obtained from the bioclimatic indicator database [53], Mozambique’s ecosystem (III) does not correspond to this assertion. The origin of this discrepancy can be attributed to the fact that other parameters must generally correct the potential evapotranspiration, such as air temperature, wind speed, vapor pressure, and the type of plant [58].

In what follows, we will use mathematical modeling

to examine the above field observations and the results obtained from remote sensing image analysis by integrating the inhomogeneities inherent in the environment of these ecosystems and changing the sign of the aridity gradient over time.

Theoretical modeling

Interaction-redistribution Model

Multiple mathematical approaches to characterize vegetation patterns have been developed as a result of the lack of physical first principles for biological and ecosystems. We use a modeling strategy where time and space are continuous so that the density of the total biomass is $b(\mathbf{r}, t)$, where $\mathbf{r} = (x, y)$ are the spatial coordinates and t is time. We use the simplest and generic ecological model [9, 59, 60]

$$\partial_t b = -\eta b + \kappa b^2 - b^3 + (d - \gamma b)\nabla^2 b - \alpha b\nabla^4 b, \quad (1)$$

where η accounts for the effective mortality rate, directly related to the natural mortality to the natality rate of vegetation, the mean annual precipitation, and water evaporation rate; it can be positive or negative. κ is called the cooperativity parameter and d accounts for the diffusion coefficient. γ and α are parameters related to interactions between neighboring plants or the water transport coupled to the vegetation dynamics. To find the definition of these parameters in terms of ecologically relevant quantities present in models, see the supplementary materials. The terms proportional to laplacian $\nabla^2 \equiv (\partial_{xx} + \partial_{yy})$ and bilaplacian $\nabla^4 \equiv (\partial_{xx} + \partial_{yy})^2$ describe diffusion and hyperdiffusion, respectively. The model Eq. [1] is derived using two different mathematical approaches where ecologically relevant parameters appear explicitly (see Supplementary Material).

We include the inhomogeneity of the environment in the parameters, promoting them to functions of space as follows $Z = Z(\mathbf{r})$, where Z could be any of the parameters $(\eta, \kappa, d, \gamma, \alpha)$. As inhomogeneities have several origins, all parameters should be considered space-dependent. We select η as a function of space. For mathematical simplicity, the remaining parameters are uniform in space. We consider spatial changes of η to be generated randomly, that is, $\eta(\mathbf{r}) = \eta + \sqrt{\Gamma}\xi(\mathbf{r})$, where $\xi(\mathbf{r})$ is a fluctuating variable of zero mean $\langle \xi(\mathbf{r}) \rangle = 0$ which has decaying radial correlations $\langle \xi(\mathbf{r})\xi(0) \rangle \propto e^{-|\mathbf{r}|/\zeta}$;

functions $\xi(\mathbf{r})$ are generated with the method described in [19]. The Γ parameter measures the intensity level of these inhomogeneities and ζ their degree of spatial correlation. Note that $\langle \eta(\mathbf{r}) \rangle = \eta$. The spatial inhomogeneities are static with respect to the timescale of biomass growth.

Pattern characteristics in homogeneous environments

If cooperativity is positive, the homogeneous equilibrium state could change abruptly to a bare state as the mortality η increases [Fig. 4a)]. Furthermore, equation [1] exhibits a regime where the system undergoes a spatial symmetry-breaking instability at $b = b_c$ to a periodic pattern with an intrinsic Fourier mode or wavenumber $q_c = \sqrt{(\gamma b_c - \delta)/(2\alpha b_c)}$, where b_c satisfies $4\alpha b_c^2(2b_c - \kappa) = (\gamma b_c - \delta)^2$. The wavelength of the vegetation patterns is $2\pi/q_c$. The η threshold at which symmetry-breaking instability occurs corresponds to $\eta_c = (\kappa - b_c^2)b_c$. Increasing η past this threshold, a classical sequence is recovered: homogeneous cover [Fig. 4b)], gaps [Fig. 4c)], rolls and labyrinths [Fig. 4d)], hexagonal patches [Fig. 4e)], and bare state. In Fig. 4a), we plot the mean biomass $\langle b \rangle = \int b(x, y)dx dy/L^2$, as a function of the η parameter for each of these states, where L is the system size. This diagram shows that adversity affects the distribution of vegetation cover and overlapping domains of stability between different types of patterns are observed. The patchy pattern survives more adverse conditions before abruptly switching to zero biomass, illustrated by the black arrow in Fig. 4a).

To analyze the spatial organization properties of numerical vegetation patterns and compare them with remote sensing data analysis, we define the binarized biomass field $A(\mathbf{r})$ of the numerical simulations as

$$A(\mathbf{r}) \equiv \begin{cases} 1 & \text{if } b(\mathbf{r}) \geq b_{sn}, \\ 0 & \text{if } b(\mathbf{r}) < b_{sn}. \end{cases} \quad (2)$$

Image and data analysis software are used to investigate the field A acquired from numerical simulations, which allows us to determine the location and size of each patch (see the supplementary materials for details). The spatial Fourier transform and the pair correlation function characterize the patch distribution. Considering a patchy hexagonal pattern as the one in Fig. 4f), extracting the main key characteristic of the patches' spatial organization is possible. The Fourier transform amplitude is

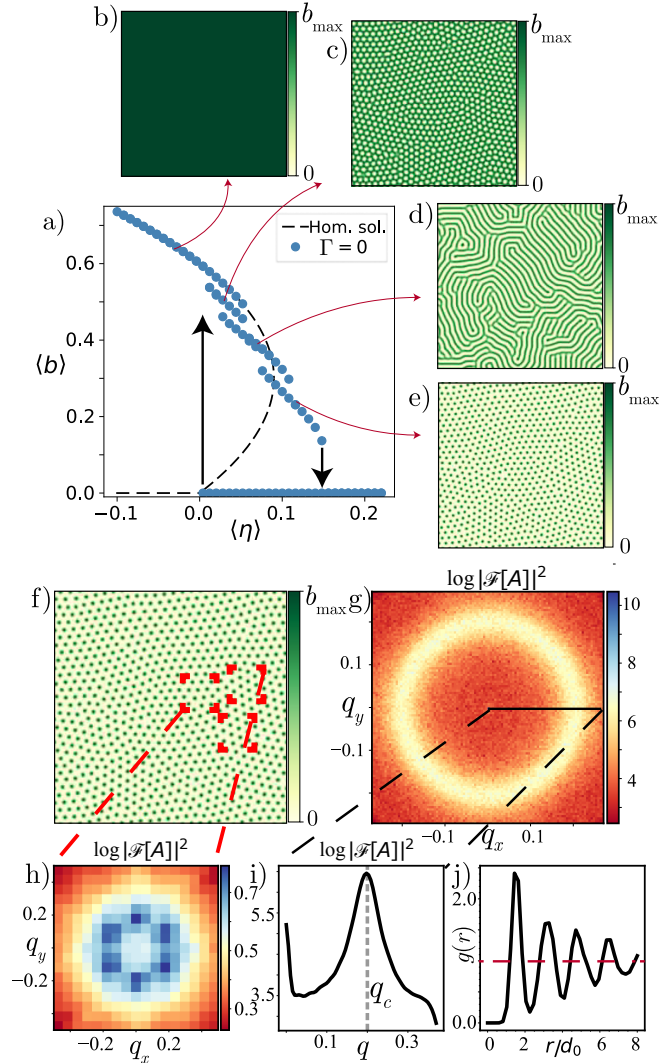


Figure 4: Bifurcation diagram of Eq. [1] for homogeneous aridity parameter obtained from numerical simulations. Parameters are $\kappa = 0.6$, $d = 0.02$, $\gamma = 0.5$, $\alpha = 0.125$. a) Bifurcation diagram of $\langle b \rangle$ vs. η , continuous (dashed) lines show stable (unstable) homogeneous equilibria, and blue dots are obtained numerically. The homogeneous cover solution becomes unstable when η increases and patterns stabilize. The transition route is b) homogeneous cover, c) hexagonal gaps, d) stripes, e) hexagonal patches, and finally, homogeneous bare soil. Note that mixed patterns can coexist for a short time in overlapping regions. f) Hexagonal patterns with some windows highlighted. g) The Fourier transform amplitude depicting a ring structure. h) Averaged random window Fourier amplitude of f), which exhibits the hexagonal (6 peaks) nature of the pattern. i) Mean radial profile of the Fourier transform amplitude showed in h). j) Pair correlation function of the patches positions

shown in Fig. 4g) and has a powdered-ring structure indicating a characteristic wavenumber. Taking random windows of A with a size comparable to the wavelength, one can unveil the type of pattern as shown in Fig. 4h),

observing six peaks in the local Fourier amplitude corresponding to a hexagonal pattern. Figure 4i) indicates the characteristic pattern wavelength $2\pi/q_c$ depicted in the mean radial profile of the Fourier transform amplitude. The corresponding pair correlation function is plotted in Fig. 4j), again indicating the presence of a periodic pattern with a well-defined wavelength. Indeed, when the environmental conditions are homogeneous, the pair correlation function has a crystalline structure, featuring peaks at defined intervals.

Inhomogeneous environmental conditions promote disordered spots by clustering

Numerical simulations of Eq. [1] with an inhomogeneous level of effective mortality η are performed using periodic boundary conditions. Figure 5 summarizes the results when using an uncorrelated inhomogeneity ($\zeta = 0$) and for a modest intensity ($\Gamma = 0.01$), we used 10 realizations of the inhomogeneity mask, with the variance among realizations being negligible; we observed that correlation length and intensity just change the width of the hysteresis loop, with no significant effect on the types of patterns observed when they are not the dominant effect, that is $\Gamma/|\eta| < 1$ and $\zeta q_c < 2\pi$. As the mean η level is increased, a branch of vegetation patterns, symbolized by the orange color, emerges from spatial instability of the homogeneous cover (dotted black curve) in Fig. 5a). The average biomass density decreases as a function of η , reaching a state of patchy pattern indicated by red dots in the diagram. An example of the obtained pattern with a high density of patches emerging from this branch is shown in Fig. 5b). An entirely distinct branch of vegetation patterns with low biomass density is observed. It emerges from covers with low density of patches when the η parameter is decreased; we refer to the vegetation pattern in this branch as clustered patches of vegetation, with the average biomass density shown in Fig. 5a) with green dots. An example of a pattern belonging to this branch is shown in Fig. 5c). The two branches form a hysteresis loop in which both vegetation patterns with a large and a small number of patches coexist for the same value η . Close to the point where the two branches with high and low biomass density meet, patches die off one by one until the system shows a gradual transition towards the bare state. Therefore, inhomogeneities can make vegetation cover more resilient to changes in envi-

ronmental conditions.

To better analyze the difference between the two branches forming a large hysteresis loop, we use the Fourier transform to show whether both branches of solutions possess a characteristic wavenumber. Figure 5b)(ii) depicts the amplitude Fourier transform of vegetation pattern shown in Fig. 5b(i), the inset shows the mean radial profile, highlighting a characteristic wavenumber q_c . A ring-like structure in the Fourier transform demonstrates that the self-organization phenomenon exhibits a characteristic wavenumber, indicating a wavelength [see, Fig. 5b)(ii)]. However, the Fourier transform of the clustered pattern, represented in Fig. 5c)(ii) loses the ring-like structure, and no defined wavelength is observed; instead, the mean radial profile of the Fourier transform decays monotonically with no local maxima as depicted in the green curve of the inset of Fig. 5c)(ii). Increasing the level of η to the point where the two branches of the solution meet leads to a random spatial distribution of patches whose positions are essentially uncorrelated. Close to this point, the characteristic wavenumber goes to zero, and the bare state becomes dominant, as shown in Fig. 5a) panel (4). It has been shown that vegetation patches could increase the system biomass by a process called self-replication [57, 61], which activates depending on the η level and the patch size. In the extreme condition of high mortality shown in Fig. 5a) panel (4), the patch self-replication process is inactive, and the patches can not invade the remaining space. However, by reversing the level of η , favorable regions due to inhomogeneities will allow the self-replication locally; different from the self-replication process in homogeneous conditions, the inhomogeneous environment will not allow complete recovery. Indeed, in this regime, inhomogeneity has a twofold effect: I) the patches that reach the critical size due to favorable local η value self-replicate, increasing the biomass of their surroundings; II) the patches will reach spatial locations with unfavorable local η , stopping the self-replicating process and pinning the colonization front. These effects, when combined, lead to a *clustering phenomenon* of patches. By further decreasing the level of mortality, more patches will be able to develop a process of self-replication, increasing the pattern density until the two branches coincide again.

In addition to the biomass involved and their Fourier space properties, a clear distinction between these two regimes can be seen in the pair correlation function plots

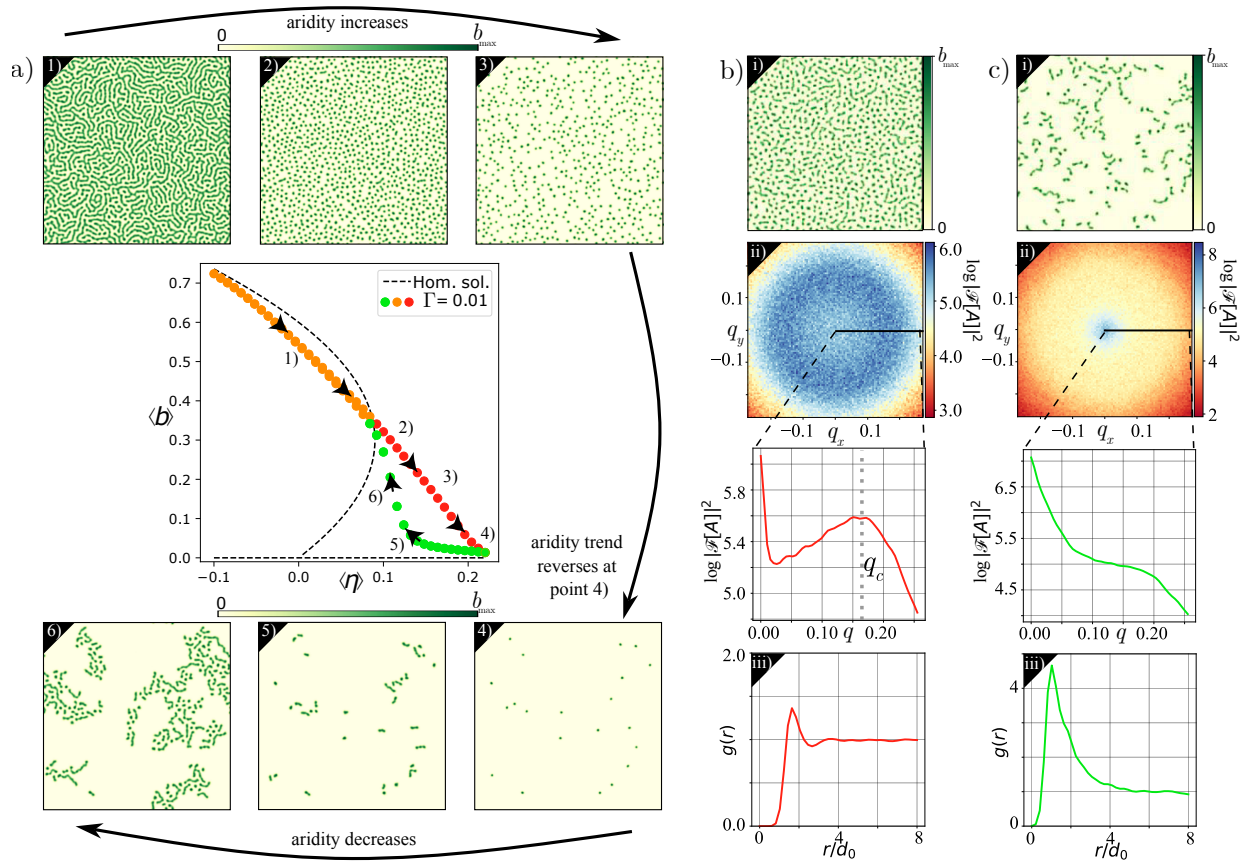


Figure 5: Numerical characterization of solution branches with heterogeneous parameters. Panel a) illustrates the bifurcation diagram for a path in the mean aridity parameter depicted by the black arrows, insets show different examples of the vegetation mosaics in the diagram. Panels b) and c) show the spatial characterization of the two branches of patchy patterns for the upper and lower branch, respectively; an example of the typical mosaic appears in i), the mean Fourier spectrum in the radial direction appears in ii), and the pair correlation function is depicted in iii). Parameters are $\kappa = 0.6$, $d = 0.02$, $\gamma = 0.5$, $\alpha = 0.125$.

of Figs. 5b)(iii) and 5c)(iii) computed for the branches of the hysteresis loop shown in the diagram Fig. 5a). As seen in Fig. 5b)(iii), the pair correlation of patches exhibits damped oscillations together with low amplitude, and the presence of a characteristic wavelength remains. The clustering process, however, reveals a greater value for the pair correlation peak that decays without any spatial order as seen in Fig. 5c)(iii).

The behavior of the two branches of solutions that are induced by inhomogeneities resembles what is observed for the spatial organization properties of the natural veg-

etation covers shown in Figs. 1 and 2. Our theory provides a possible explanation for these field observations with the least ingredients to produce these emergent behaviors: inhomogeneous parameters acting over mathematical models of vegetation self-organization. Patchy vegetation patterns in Fig. 2 from (i) to (iv) could be classified as states with no pattern structure and the same properties as cover from the lower branch of the diagram in Fig. 5a), whereas cover in Fig. 2 from (v) to (viii) could be classified as states with a pattern structure and properties similar to the upper branch of the

diagram shown in Fig. 5a). This vegetation cover classification could allow us to infer possibilities for the history of the biomass and the η parameter.

Conclusions

To conclude, we studied the formation of vegetation patterns in arid and semi-arid zones using field observations and remote sensing image analysis, as well as mathematical modeling considering inhomogeneities in the parameters that could be produced by spatial soil irregularities, interannual precipitation fluctuations, fire occurrences, grazing, soil depth distribution, and soil-moisture islands. The following results were obtained:

- Field observations and remote sensing image analysis based solely on two-dimensional Fourier image analysis, combined with a pairwise correlation function, enabled us to classify several vegetation patches under irregularities in the topography. Two processes were identified: self-organization and clustering. Self-organization with a well-defined wavelength emerges as the level of aridity increases. We have shown that this process results from increasing aridity levels. In contrast, clustering processes emerge when the aridity gradient is reversed, and the resulting pattern loses its wavelength.
- Using a database of bio-climatic indicators allowed us to extract the aridity spatiotemporal behavior using two bioclimatic quantities: the mean annual precipitation and the reference potential evapotranspiration. This allowed us to predict that the ecosystem will exhibit self-organization as a result of aridity increases or, on the contrary, will undergo a clustering process thanks to aridity reduction. We established the global trend map to indicate possible ecosystems' self-organization and clustering.
- Using mathematical modeling, we have shown that in the absence of spatial irregularities, ecosystems undergo catastrophic changes toward a bare state. All patches disappear at some point when an effective mortality threshold is exceeded. However, if spatial irregularities are taken into account, the patch ecosystem shows a rather gentle,

gradual transition. In addition, we have identified two branches associated with self-organization and clustering of vegetation patches. These two branches form a hysteresis loop for a wide range of the effective mortality parameter and are only observed when environmental inhomogeneities are taken into account.

The correspondence between the classification of the vegetation patterns and the history of the aridity parameter can be a useful indicator for landscape degradation and recovery. This observation is in good agreement with theoretical predictions showing a hysteresis loop between self-organization and clustering. Based solely on the evolution of the aridity parameter, we have proposed a simple criterion to show whether the ecosystem is developing self-organization or clustering. With the use of statistical tools for spatial analysis and numerical simulations of the governing equations, our results represent a step toward a practical, non-destructive method for classifying vegetation patterns and predicting their behavior.

Conflict of interest

The authors declare that they have no conflict of interest regarding this work.

Acknowledgments

The authors thank S. Echeverria for fruitful discussions. D.P.-R. acknowledges the financial support of ANID National Ph.D. Scholarship 2020-21201484. M.G.C. acknowledges the financial support of ANID-Millennium Science Initiative Program-ICN17_012 (MIRO) and FONDECYT project 1210353. M.T. is a Research Director at Fonds de la Recherche Scientifique FNRS. We would also like to thank the CNRST for its support under the FINCOME programme (N L71/2022).

Author contributions

DPR, MGC, and MT conceptualized the work. All the authors wrote, revised, and accorded the final version of the manuscript. DPR performed the data analysis and numerical simulations. AM collected the on-site data by smart drone scanning in the Morocco ecosystem.

References

- [1] René Lefever and Olivier Lejeune. On the origin of tiger bush. *Bulletin of Mathematical biology*, 59(2):263–294, 1997.
- [2] Christopher A Klausmeier. Regular and irregular patterns in semiarid vegetation. *Science*, 284(5421):1826–1828, 1999.
- [3] Reinier HilleRisLambers, Max Rietkerk, Frank van den Bosch, Herbert HT Prins, and Hans de Kroon. Vegetation pattern formation in semi-arid grazing systems. *Ecology*, 82(1):50–61, 2001.
- [4] Jost von Hardenberg, Ehud Meron, Moshe Shachak, and Yair Zarmi. Diversity of vegetation patterns and desertification. *Physical review letters*, 87(19):198101, 2001.
- [5] Paolo D’Odorico, Francesco Laio, and Luca Ridolfi. Patterns as indicators of productivity enhancement by facilitation and competition in dryland vegetation. *Journal of Geophysical Research: Biogeosciences*, 111(G3), 2006.
- [6] Vincent Deblauwe, Pierre Couteron, Olivier Lejeune, Jan Bogaert, and Nicolas Barbier. Environmental modulation of self-organized periodic vegetation patterns in sudan. *Ecography*, 34(6):990–1001, 2011.
- [7] Miguel Berdugo, Manuel Delgado-Baquerizo, Santiago Soliveres, Rocío Hernández-Clemente, Yanchuang Zhao, Juan J Gaitán, Nicolas Gross, Hugo Saiz, Vincent Maire, Anika Lehmann, et al. Global ecosystem thresholds driven by aridity. *Science*, 367(6479):787–790, 2020.
- [8] Weigang Hu, Jinzhi Ran, Longwei Dong, Qiajun Du, Mingfei Ji, Shuran Yao, Yuan Sun, Chunmei Gong, Qingqing Hou, Haiyang Gong, et al. Aridity-driven shift in biodiversity–soil multifunctionality relationships. *Nature communications*, 12(1):5350, 2021.
- [9] Olivier Lejeune and Mustapha Tlidi. A model for the explanation of vegetation stripes (tiger bush). *Journal of Vegetation science*, 10(2):201–208, 1999.
- [10] Olivier Lejeune, Mustapha Tlidi, and René Lefever. Vegetation spots and stripes: dissipative structures in arid landscapes. *International journal of quantum chemistry*, 98(2):261–271, 2004.
- [11] Max Rietkerk, Maarten C Boerlijst, Frank van Langevelde, Reinier HilleRisLambers, Johan van de Koppel, Lalit Kumar, Herbert HT Prins, and André M de Roos. Self-organization of vegetation in arid ecosystems. *The American Naturalist*, 160(4):524–530, 2002.
- [12] Paolo D’Odorico, Amilcare Porporato, and Christiane Wilkinson Runyan. *Dryland ecohydrology*, volume 9. Springer, 2006.
- [13] Olivier Lejeune, Mustapha Tlidi, and Pierre Couteron. Localized vegetation patches: a self-organized response to resource scarcity. *Physical Review E*, 66(1):010901, 2002.
- [14] Max Rietkerk, Stefan C Dekker, Peter C De Ruiter, and Johan van de Koppel. Self-organized patchiness and catastrophic shifts in ecosystems. *Science*, 305(5692):1926–1929, 2004.
- [15] Marcel Gabriel Clerc, S Echeverría-Alar, and Mustapha Tlidi. Localised labyrinthine patterns in ecosystems. *Scientific reports*, 11(1):1–12, 2021.
- [16] Mustapha Tlidi, MG Clerc, Daniel Escaff, Pierre Couteron, M Messaoudi, M Khaffou, and Abdelakader Makhoute. Observation and modelling of vegetation spirals and arcs in isotropic environmental conditions: dissipative structures in arid landscapes. *Philosophical Transactions of the Royal Society A: Mathematical, Physical and Engineering Sciences*, 376(2135):20180026, 2018.
- [17] Daniel Ruiz-Reynés, Elvira Mayol, Tomàs Sintes, Iris E Hendriks, Emilio Hernández-García, Carlos M Duarte, Núria Marbà, and Damià Gomila. Self-organized sulfide-driven traveling pulses shape seagrass meadows. *Proceedings of the National Academy of Sciences*, 120(3):e2216024120, 2023.
- [18] Belen Hidalgo, David Pinto, Mustapha Tlidi, and Marcel Clerc. Nonreciprocal feedback induces migrating oblique and horizontal banded vegetation patterns in hyperarid landscapes. 2024.

- [19] D Pinto-Ramos, S Echeverría-Alar, Marcel Gabriel Clerc, and Mustapha Tlidi. Vegetation covers phase separation in inhomogeneous environments. *Chaos, Solitons & Fractals*, 163:112518, 2022.
- [20] Koen Siteur, Quan-Xing Liu, Vivi Rottschäfer, Tjisse van der Heide, Max Rietkerk, Arjen Doelman, Christoffer Boström, and Johan van de Koppel. Phase-separation physics underlies new theory for the resilience of patchy ecosystems. *Proceedings of the National Academy of Sciences*, 120(2):e2202683120, 2023.
- [21] Pierre Couteron. Conservative or dissipative? two distinct processes for spatial pattern emergence. *Proceedings of the National Academy of Sciences*, 120(5):e2221117120, 2023.
- [22] S Echeverría-Alar, D Pinto-Ramos, M Tlidi, and MG Clerc. Effect of heterogeneous environmental conditions on labyrinthine vegetation patterns. *Physical Review E*, 107(5):054219, 2023.
- [23] H Yizhaq, S Sela, T Svoray, S Assouline, and G Bel. Effects of heterogeneous soil-water diffusivity on vegetation pattern formation. *Water Resources Research*, 50(7):5743–5758, 2014.
- [24] Hezi Yizhaq and Golan Bel. Effects of quenched disorder on critical transitions in pattern-forming systems. *New Journal of Physics*, 18(2):023004, 2016.
- [25] Hezi Yizhaq, Ilan Stavi, Moshe Shachak, and Golan Bel. Geodiversity increases ecosystem durability to prolonged droughts. *Ecological Complexity*, 31:96–103, 2017.
- [26] Natalie De Falco, Reut Tal-Berger, Amgad Hjazin, Hezi Yizhaq, Ilan Stavi, and Shimon Rachmilevitch. Geodiversity impacts plant community structure in a semi-arid region. *Scientific reports*, 11(1):15259, 2021.
- [27] Uri Basson, Eli Argaman, Hezi Yizhaq, Chi Xu, Zhiwei Xu, and Ilan Stavi. Subsurface geodiversity determines shrub resilience vs. mortality under long-term droughts in the israeli negev drylands. *Frontiers in Environmental Science*, 2023.
- [28] Gavan S McGrath, Kyungrock Paik, and Christoph Hinz. Microtopography alters self-organized vegetation patterns in water-limited ecosystems. *Journal of Geophysical Research: Biogeosciences*, 117(G3), 2012.
- [29] Punit Gandhi, Lucien Werner, Sarah Iams, Karna Gowda, and Mary Silber. A topographic mechanism for arcing of dryland vegetation bands. *Journal of The Royal Society Interface*, 15(147):20180508, 2018.
- [30] Trenton E Franz, Elizabeth G King, Kelly K Caylor, and David A Robinson. Coupling vegetation organization patterns to soil resource heterogeneity in a central kenyan dryland using geophysical imagery. *Water resources research*, 47(7), 2011.
- [31] Ignacio Rodriguez-Iturbe, Zijuan Chen, Ann Carla Staver, and Simon Asher Levin. Tree clusters in savannas result from islands of soil moisture. *Proceedings of the National Academy of Sciences*, 116(14):6679–6683, 2019.
- [32] P Adler, D Raff, and W Lauenroth. The effect of grazing on the spatial heterogeneity of vegetation. *Oecologia*, 128(4):465–479, 2001.
- [33] Paolo D’Odorico, Francesco Laio, Amilcare Porporato, Luca Ridolfi, and Nicolas Barbier. Noise-induced vegetation patterns in fire-prone savannas. *Journal of Geophysical Research: Biogeosciences*, 112(G2), 2007.
- [34] SR Tega II, Ivric Valaire Yatat-Djeumen, Jean Jules Tewa, and Pierre Couteron. Spatio-temporal modelling of tree-grass dynamics in humid savannas: Interplay between nonlocal competition and non-local facilitation. *Applied Mathematical Modelling*, 104:587–627, 2022.
- [35] Yanfen Wang, Kai Xue, Ronghai Hu, Boyang Ding, Hong Zeng, Ruijin Li, Bin Xu, Zhe Pang, Xiaoning Song, Congjia Li, et al. Vegetation structural shift tells environmental changes on the tibetan plateau over 40 years. *Science Bulletin*, 68(17):1928–1937, 2023.
- [36] Paolo D’Odorico, Francesco Laio, and Luca Ridolfi. Vegetation patterns induced by random cli-

- mate fluctuations. *Geophysical Research Letters*, 33(19), 2006.
- [37] Paula Villa Martín, Juan A Bonachela, Simon A Levin, and Miguel A Muñoz. Eluding catastrophic shifts. *Proceedings of the National Academy of Sciences*, 112(15):E1828–E1836, 2015.
- [38] Marten Scheffer, Steve Carpenter, Jonathan A Foley, Carl Folke, and Brian Walker. Catastrophic shifts in ecosystems. *Nature*, 413(6856):591–596, 2001.
- [39] Sonia Kéfi, Max Rietkerk, Concepción L Alados, Yolanda Pueyo, Vasilios P Papanastasis, Ahmed ElAich, and Peter C De Ruiter. Spatial vegetation patterns and imminent desertification in mediterranean arid ecosystems. *Nature*, 449(7159):213–217, 2007.
- [40] Vasilis Dakos, Sonia Kéfi, Max Rietkerk, Egbert H Van Nes, and Marten Scheffer. Slowing down in spatially patterned ecosystems at the brink of collapse. *The American Naturalist*, 177(6):E153–E166, 2011.
- [41] D Pinto-Ramos, MG Clerc, and M Tlidi. Topological defects law for migrating banded vegetation patterns in arid climates. *Science Advances*, 9(31):eadf6620, 2023.
- [42] Max Rietkerk, Robbin Bastiaansen, Swarnendu Banerjee, Johan van de Koppel, Mara Baudena, and Arjen Doelman. Evasion of tipping in complex systems through spatial pattern formation. *Science*, 374(6564):eabj0359, 2021.
- [43] Ernesto Berríos-Caro, Marcel Gabriel Clerc, Daniel Escaff, C Sandivari, and Mustapha Tlidi. On the repulsive interaction between localised vegetation patches in scarce environments. *Scientific reports*, 10(1):1–8, 2020.
- [44] NASA JPL, 2013. NASA Shuttle Radar Topography Mission Global 1 arc second [Data set]. NASA EOSDIS Land Processes DAAC. Accessed 2022-12-01 from <https://doi.org/10.5067/MEaSURES/SRTM/SRTMGL1.003>.
- [45] Borja Rodríguez-Lozano, Emilio Rodríguez-Caballero, Lisa Maggioli, and Yolanda Cantón. Non-destructive biomass estimation in mediterranean alpha steppes: Improving traditional methods for measuring dry and green fractions by combining proximal remote sensing tools. *Remote Sensing*, 13(15):2970, 2021.
- [46] Christian Körner and Christian Kèorner. *Alpine plant life: functional plant ecology of high mountain ecosystems*. Springer, Berlin, 1999, 1999.
- [47] Fabien Anthelme and Olivier Dangles. Plant–plant interactions in tropical alpine environments. *Perspectives in Plant Ecology, Evolution and Systematics*, 14(5):363–372, 2012.
- [48] Ricardo Martinez-Garcia, Ciro Cabal, Justin M Calabrese, Emilio Hernández-García, Corina E Tarnita, Cristóbal López, and Juan A Bonachela. Integrating theory and experiments to link local mechanisms and ecosystem-level consequences of vegetation patterns in drylands. *Chaos, Solitons & Fractals*, 166:112881, 2023.
- [49] Nicolas Barbier, Pierre Couteron, René Lefever, Vincent Deblauwe, and Olivier Lejeune. Spatial decoupling of facilitation and competition at the origin of gapped vegetation patterns. *Ecology*, 89(6):1521–1531, 2008.
- [50] René Lefever, Nicolas Barbier, Pierre Couteron, and Olivier Lejeune. Deeply gapped vegetation patterns: on crown/root allometry, criticality and desertification. *Journal of Theoretical Biology*, 261(2):194–209, 2009.
- [51] René Lefever and John W Turner. A quantitative theory of vegetation patterns based on plant structure and the non-local f-kpp equation. *Comptes Rendus Mécanique*, 340(11-12):818–828, 2012.
- [52] Pierre Couteron, Fabien Anthelme, Marcel Clerc, Daniel Escaff, Cristian Fernandez-Oto, and Mustapha Tlidi. Plant clonal morphologies and spatial patterns as self-organized responses to resource-limited environments. *Philosophical Transactions of the Royal Society A: Mathematical, Physical and Engineering Sciences*, 372(2027):20140102, 2014.

- [53] H. Wouters, J. Berckmans, R. Maes, E. Vanuytrecht, and K. De Ridder. Global bioclimatic indicators from 1979 to 2018 derived from reanalysis, 2021. version 1.0, Copernicus Climate Change Service (C3S) Climate Data Store (CDS), (Accessed on 05-06-2022), DOI: 10.24381/cds.bce175f0.
- [54] M Tlidi, M Messaoudi, A Makhoute, D Pinto-Ramos, and MG Clerc. Non-linear and non-local plant-plant interactions in arid climate: Allometry, criticality and desertification. *Chaos, Solitons & Fractals*, 178:114311, 2024.
- [55] Fabio Borgogno, P D’Odorico, Francesco Laio, and Luca Ridolfi. Mathematical models of vegetation pattern formation in ecohydrology. *Reviews of geophysics*, 47(1), 2009.
- [56] S Echeverría-Alar and MG Clerc. Labyrinthine patterns transitions. *Physical Review Research*, 2(4):042036, 2020.
- [57] Ignacio Bordeu, Marcel G Clerc, Piere Couteron, René Lefever, and Mustapha Tlidi. Self-replication of localized vegetation patches in scarce environments. *Scientific reports*, 6(1):1–11, 2016.
- [58] John L Monteith. Evaporation and environment. In *Symposia of the society for experimental biology*, volume 19, pages 205–234. Cambridge University Press (CUP) Cambridge, 1965.
- [59] Mustapha Tlidi, René Lefever, and Andrei Vladimirov. On vegetation clustering, localized bare soil spots and fairy circles. In *Dissipative Solitons: From Optics to Biology and Medicine*, pages 1–22. Springer, 2008.
- [60] Daniel Ruiz-Reynés, Francesca Schönsberg, Emilio Hernández-García, and Damià Gomila. General model for vegetation patterns including rhizome growth. *Physical Review Research*, 2(2):023402, 2020.
- [61] Mustapha Tlidi, Ignacio Bordeu, Marcel G Clerc, and Daniel Escaff. Extended patchy ecosystems may increase their total biomass through self-replication. *Ecological indicators*, 94:534–543, 2018.